Experimental Investigation and Kinetic Modeling of Naphtha Catalytic Reforming Using Pt-Re/Al_2O_3 Catalyst

Rasaei, Yasaman; Towfighi Darian, Jafar
Faculty of Chemical Engineering, Tarbiat Modares University, Tehran, I.R. IRAN

Royaee, Sayed Javid*[+]
Petroleum Refining Technology Development Division, Research Institute of Petroleum Industry, Tehran, I.R. IRAN

ABSTRACT: *Catalytic reforming is a process known in the refining industry to improve the quality of gasoline by increasing the octane number, the production of aromas, and hydrogen production as a byproduct. The purpose of this research is to develop a kinetic model for naphtha catalytic reforming reactions with consideration of simple and reliable assumptions and also to provide a mathematical model using mass balance. In the kinetic model, 22 lamps and 48 reactions are present. Also, in the mathematical model, the superficial velocity of the fluid is considered variable in the axial direction of the reactor. In order to evaluate the proposed model, laboratory tests have been used in 24 different operating conditions, which according to the results of the analysis of the products, the yield of liquid is observed in the range of 0.701 to 0.952. Also, using experimental results, the model parameters are obtained through optimization with MATLAB software. Finally, the results of comparing the predicted product distribution through the model with their experimental values showed that the proposed model with acceptable accuracy could predict the distribution of the products.*

KEYWORDS: *Catalytic naphtha reforming; Kinetic modeling; Optimization.*

INTRODUCTION

Although the burning of any kind of fossil fuels plays a major role in releasing carbon dioxide and other toxic gases into environmental problems, it is still the most important source of energy in the world. In order to preserve the environment, various measures have been taken, including increasing the number of octane in gasoline fuels [1]. Today, the naphtha reforming process is one of the most advanced processes in the refining industry. Naphtha catalytic reforming is a combination of catalyst and hardware technologies and process complexity that result from high-octane reformate to produce gasoline or aromatics as feedstock for petrochemicals [2]. Naphtha is a fraction of crude oil, approximately %15-30 by weight of crude oil, with a boiling range of 30-200°C, and includes various hydrocarbon groups such as paraffin (alkanes), naphtene (cycloalkanes), and aromatics with 5 to 12 carbon atoms, sulfur, and nitrogen as impurity [3]. The presence of sulfur

* *To whom correspondence should be addressed.*
+ E-mail: royaeesj@ripi.ir ; royaeesj@gmail.com
1021-9986/2021/1/275-287 13/$/6.03

in naphtha has a negative effect on the performance of catalysts. Sulfur compounds in fuels are a global problem that causes environmental problems and air quality. Therefore, in order to prevent the negative effects of sulfur, naphtha feed is desulfurized in HDS unit before entering to reforming unit [4]. The goal of the catalytic reforming process is to convert the naphtha with low quality and octane number to high-octane gasoline. This process is also one of the main sources of Benzene, Toluene, Xylene (BTX) aromatics. During this process, significant amounts of hydrogen are produced, which is used in other refinery units [5]. The naphtha catalytic reforming process is divided into two process groups with fixed bed and moving bed reactors. Semi-regenerative and cyclic units are considered as two main and important types of fixed bed reactors. On the other hand, moving bed reactors operate in a continuous regenerative process. In sum, the continuous regenerative process can produce products with higher octane numbers. The continuous regeneration is preferred from other aspects, such as high catalyst activity and fewer requirements, more uniform reformate with higher aromatic content, and higher hydrogen purity than other catalyst recovery processes. Therefore, the modern designs of naphtha reforming reactors are based on this type [6,7]. In this process, there are three reactors in series. Of course, in some industrial cases, four series reactors are used. These reactors are not the same size, and usually, the first reactor has the smallest and the last reactor of the largest size [8]. Various reactions are taking place in these reactors, the most important of which are dehydrogenation, dehydrocyclization, isomerization, hydrocracking, hydrodealkylation, and formation of coke [9]. Dehydrogenation, dehydrocyclization, and isomerization are the desired reactions because they control the octane number and hydrogen purity. In contrast, hydrocracking is undesirable because it cracks paraffins into smaller paraffins that produce light gases (lower octane, LPG). The formation of coke is also considered to be a bad reaction due to its negative effect on catalyst activity [10]. Variables that influence the performance of the catalyst, the change in the yield, and product quality in terms of octane number are feed properties, reaction temperature, reaction pressure, weighted hourly space velocity, and the molar ratio of hydrogen to hydrocarbons [11].

Studies in the field of this process are divided into three categories. The first batch of studies is on improving the operation, selectivity of the catalyst, and reducing the formation of coke on the surface of the catalyst by adding a series of metal-based catalysts. The second group studies the kinetic model. In order to reduce the complexity caused by the multiplicity of components and reactions, similar chemical components are placed in a group and a lump. The final category of studies on reforming processes relates to reactor modeling and implementation of a new and optimal operational structure [12].

Considering the importance of the kinetic models in industrial design, many kinetic models with different conditions and assumptions for the naphtha catalytic reforming process have been presented. The hypothesis of the lump-in kinetic models has been able to facilitate modeling while having reliable accuracy. The first effective effort to provide a lumped model for the reforming system was carried out by *Smith*. His model, which is the simplest model, consists of three main types of compounds: paraffin, naphthene, and aromatics, which were subjected to four reactions [13]. *Krane* and *Colleagues* considered more hydrocarbons. In his model, most of the basic reactions, except for, were present [14]. *Padmavathia* and *colleagues* presented a more detailed model with the presence of various PAN isomers. The reaction pathway for six-carbon hydrocarbons was also carefully evaluated [15]. In recent years, more researchers, including *Rodriguez* and *Colleagues* [5], *Iranshahi* and *Colleagues* [12], *Zagoruiko et al.* [16] have been active in this field. In most studies, kinetic parameters have been obtained with the help of industrial information, or empirical data of other articles has been used. In previous studies, fluid velocity has been assumed to be constant in a reactor.

The purpose of this research is to develop a kinetic model for the naphtha catalytic reforming reactions. The present model is based on Krane's model [14] and with more precise assumptions in the form of 22 lumps and 48 reactions. Noteworthy in this paper is the hypothesis of the variable superficial velocity of the fluid inside the reactor, which is taken into account in kinetic modeling due to molecular variations due to chemical reactions. The kinetic parameters of this model are obtained using the results of analyzes of the laboratory tests of the naphtha catalytic reforming process and also using the MATLAB software optimization tool. Finally, the difference between the predicted concentrations of hydrocarbons by model and their experimental values is obtained.

EXPERIMENTAL SECTION

Material and Equipment

In order to obtain the experimental values of the distribution of products on a laboratory scale, the corresponding tests have been carried out. Process feed is desulfurized heavy naphtha from the Tehran Refinery's CRU unit and the industrial catalyst used, is based on alumina (Pt-Re / Al_2O_3) platinum rhenium. Hydrogen, air, and nitrogen capsules are also used to prepare and set up the laboratory system. The naphtha catalytic reforming process is carried out in a fixed tube bed reactor with an inner diameter of 3.2 cm and the final product is obtained by passing the flash separator in two phases of gas and liquid. Among other equipment used include the circulator, the furnace, the pressure control valve, the material flow controller and the thermocouple.

Experimental proceedings

Prior to the preparation of the laboratory system, ASTM D86 analysis, DHA analysis, and Total Sulfur analysis, and Karl Fisher's test for determining the amount of water in the feed were performed. Table 1 summarizes the results of these analyzes and catalyst specifications. After reviewing the optimal industrial conditions, the operating conditions for laboratory tests according to the industrial ranges are selected in the form of 24 main tests and are presented in Table 2.

It is worth noting that for applying WHSV for values of 1, 2, and 5 h^{-1} of this parameter, values of 50, 25 and 10 grams of catalyst are used, and the inlet mass flow of naphtha and hydrogen is constant at 50 g/h and 5.62 g/h. The length of the reaction bed for the values of 50, 25, and 10 grams of the catalyst has a height of 8.8, 4.4, and 1.76 cm. Therefore, the density of the bed is 706.83 kg cat /m^3.

To prepare the laboratory system, the following procedures are taken:

Grinding and curing of the catalyst, filling the reactor entrance section with a welding stone to create better dispersion in the bed, drying the catalyst to eliminate the probable absorption of water and maintaining the acidity of the catalyst using chlorine and oxygen, reduction of the catalyst to free the metal site by adding hydrogen and sulfurizing catalyst. The setup is ready for the main tests, and 24 basic tests are taken in the designated operating conditions. Liquid and gaseous samples are analyzed using the GC device.

After completion of the main tests, two other tests were conducted to investigate the main mechanism of the ring reaction by preparing synthetic feed containing 20% vol. pentane (P5), 35% hexane (P6), 45% heptane (P7) under operating conditions, H_2/ Oil = 6, temperature 470°C, pressure 15 bar and WHSV= 1 and 5 hr^{-1}.

KINETIC MODELING SECTION

Due to the very low-pressure drop across the reactor, the constant velocity hypothesis can be an acceptable hypothesis in the mass balance equations, as used in past works. But it should be noted that along the reactor, there are a lot of chemical reactions and the number of moles changes. The change in mole leads to a change in fluid volume. The reactor is a tube reactor with a constant cross-section. So, by changing the volume of the fluid in this type of reactor, the fluid velocity in the output is variable. Therefore, the variable velocity hypothesis is more accurate than the constant velocity in equations.

Mass balance equation

Using hypotheses and mass balance equations, a mathematical model is presented and then a reaction network is developed based on the lump hypothesis. The basis of the work of mathematical modeling is the transfer phenomenon equations. In order to reduce the complexity, a series of simplistic assumptions are used which, while simplifying, have an acceptable degree of accuracy.

- Ideal gas law
- One-dimensional modeling in the axial direction
-Isothermal system and constant temperature, regardless of pressure drop in the axial direction due to low height
- The superficial velocity of the fluid variable inside the reactor; due to changes in the mole and, consequently, the volume changes resulting from chemical reactions as well as the constant cross-section
- The introduction of fluid into a catalytic bed in a fully developed state
- steady-state conditions
- Avoid the transmission of mass diffusion in the axial direction
- Regardless of the stresses created in the axial direction
- Regardless of the catalyst deactivation due to the short duration of use of the catalyst

Table 1: Results of elementary analyses of feed and typical properties of catalyst.

Distillation fraction of naphtha feed		
ASTM D86	Naphtha feed (°C)	
IBP	82	
5%	92	
10%	98	
20%	102	
30%	105	
40%	110	
50%	112	
60%	116	
70%	120	
80%	128	
90%	138	
95%	144	
FBP	165	
Total sulfur	nil	
Content of water	17 ppm wt	
Density of feed	723 kg/m^3	
Typical properties of the catalyst		
d_p	1.6	mm
a_s	220	m^2/g
v_p	0.6	cm^3/g
Al_2O_3	89.01	wt%
Pt	0.3	wt%
Re	0.4	wt%

Table 2: Operating conditions of experiments.

Temperature (°C)	470	480	490	500
WHSV (h^{-1})	1	2	5	
Pressure (barg)	10	15		
H_2/Oil	6			

- Plug flow pattern according to operating temperature and pressure conditions.

Energy balance equations are not applicable to modeling with respect to the constant temperature hypothesis and isothermal system. On the other hand, due to the absence of a term of change in momentum due to chemical reactions in the classical momentum equations, these equations cannot play a role in considering the velocity variations in the model. Now based on the above assumptions, mass balance equations are presented.

$$\frac{\partial C_j}{\partial z} = -\frac{C_j}{U_z}\cdot\frac{\partial U_z}{\partial z} + \frac{\rho_B}{U_z}\sum_{i=1}^{m} V_{ij} r_i \quad (1)$$

$$\frac{\partial U_z}{\partial z} = \frac{\rho_B}{U_z}\sum_{j=1}^{n}\sum_{i=1}^{m} V_{ij} r_i \quad (2)$$

Kinetic modeling

Most models are based on the lump's hypothesis and report the rate constants. The complexity level of these models varies from low lump count to kinetic models with great detail [5]. In line with the purpose of this research, the model is based on the model of lump and reference [14]. But with surveys and studies from other sources and references, some of the reactions in the base model, which are less likely to occur, have been removed, and more probable assumptions have been replaced for the kinetic model. It is anticipated that this hypothesis can largely fit the laboratory information and properly represent the distribution of products. Under the assumptions below, the reaction matrix and their rate equations are defined:

- In this model, three main hydrocarbons include paraffins with carbon atoms of 1 to 10, naphthens and aromatics with carbon atoms of 6 to 10, and hydrogen in the form of 22 lumps. Only 6 carbon naphthene with two isomers, cyclohexane, and methylcyclopentane, are divided into two separate lumps. These isomers are not present in the original model.

- Rate equations of reactions are first order. Due to the high concentration of hydrogen compared to other feed compounds, the concentration of hydrogen with a rate constant is integrated.

- In paraffin cyclization reaction, referring to reference [17], the transformation of paraffin into naphtha is more likely than the direct route of paraffin to aromatics. Due to the role of naphthene as an intermediate between paraffin to aromatics, less activation energy is required. Experimental and laboratory results also confirm this.

- In the cyclization reaction of 6-carbon paraffin (P6), the only methylcyclopentane is produced from 6 carbon naphthene. Since these isomers are not present in the base model, this hypothesis does not exist.

- The opening naphthenic ring reaction (backward path of cyclization reaction) is included in this model. In this reaction, contrary to the reaction of ringing, both types of naphthene isomer 6 carbon (methylcyclopantane and cyclohexane) participate in this reaction.

- One of the main reactions is the hydrocracking of paraffins. In this reaction, heavy paraffins produce all the paraffins with less atomic number than themselves.

- The isomerization reaction is considered merely for the 6 carbon naphthenes and between the two isomers of methylcyclopentane and cyclohexane. While this reaction is not seen in the original model.

- The dehydrogenation reaction, the conversion of naphthene to aromatics, is the fastest reaction of this process. Unlike the base model, which considers the only forward path of dehydrogenation, this model has both the forward and backward reactions of dehydrogenation. Also, only cyclohexane from 6 carbon naphthenic isomers is converted into benzene and methylcyclopentane does not participate in this reaction. On the other hand, the benzene ring only reacts to the cyclohexane isomer.

- Hydrodealkylation reaction is one of the reactions that are of interest to this model. Referring to reference [17], heavier aromatics go on to produce toluene (A_7) because of the stability of the benzyl ring.

According to the above assumptions, the reaction matrix, which contains 48 reactions, is schematically shown in Fig. 1.

RESULTS AND DISCUSSION

Examining experimental results

Analysis of gas and liquid products is done with GC device. The results of the analysis of liquid products in Table 3 are based on the percentage of paraffin (P), naphthene (N), and aromatic (A) in each of the 24 main tests and two synthesis tests.

According to Table 3, the amounts of paraffin and naphthenic compounds in products have decreased due to consumption in reactions such as dehydrocyclization and dehydrogenation, and in contrast to the amounts of aromatic compounds increased in response to desired reactions.

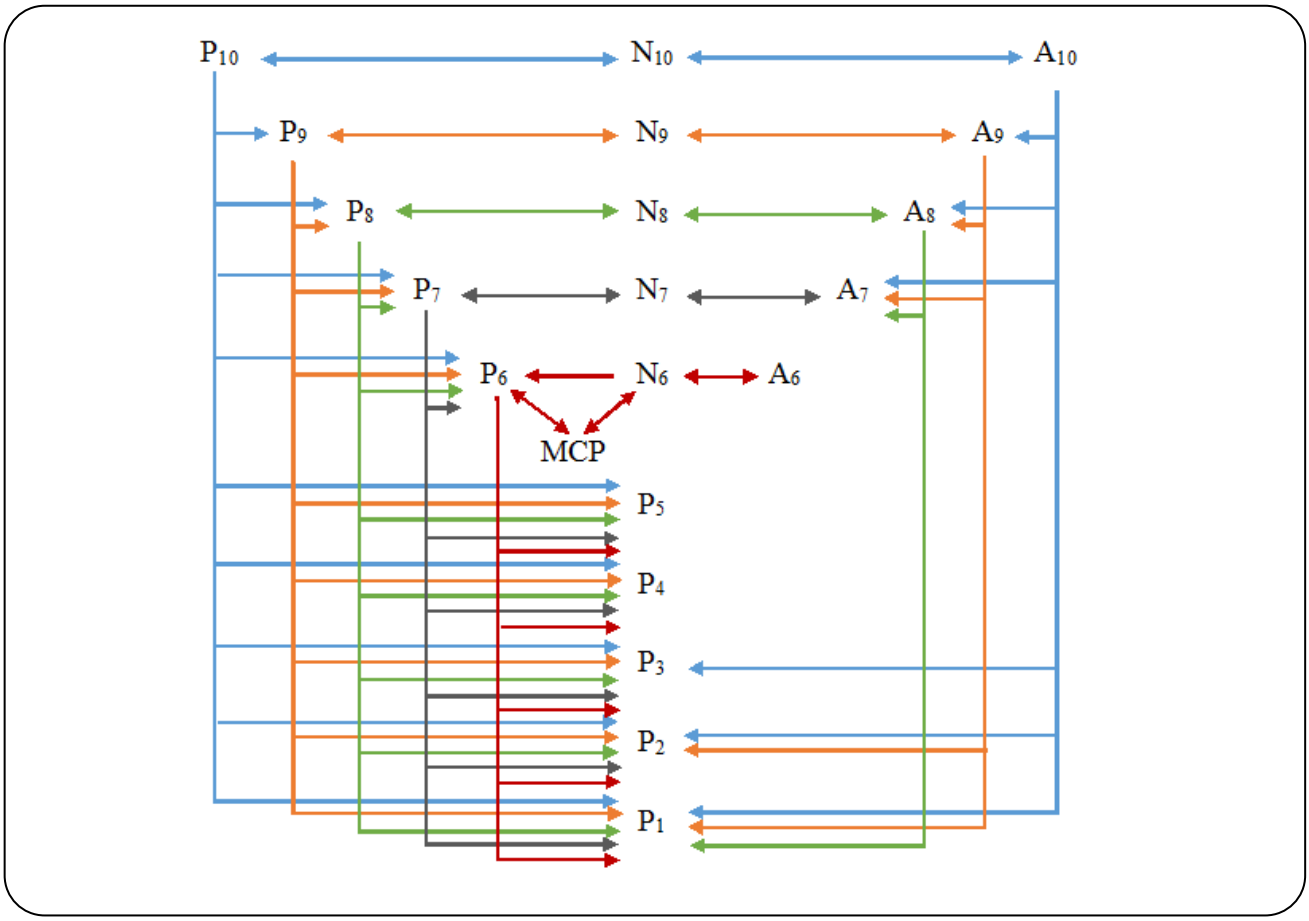

Fig. 1: Reaction network scheme for the naphtha reforming process.

By increasing the temperature from 470°C to 500°C and the constant of other parameters, paraffin and naphthenic compounds have been consumed more and aromatic production has increased. This means that the increase in temperature leads to an increase in the conversion rate of the desired product and at the temperature of 500°C the most aromatic production is observed.

On the other hand, by comparing the results of analyzes at two pressures of 15 and 10 bar and the constant of other parameters, it is observed that at a lower pressure (10 bar), the aromatic production increased due to the higher consumption of paraffin and naphthene.

The WHSV parameter represents the contact time of feed with the catalyst. According to Table 3, under constant conditions, the amount of aromatic production decreased by increasing the WHSV from 1 to 5 h^{-1} (actually reducing the residence time). And in WHSV=1 h^{-1} the highest amount of aromatic conversion is observed.

In the results of the synthetic feed test, it can be seen that the final product of the process with synthetic feed, including P_5, P_6, P_7, in the WHSV=1 h^{-1}, contain 80.81% mole paraffin, 14.46 % mole naphthene, and 4.23% mole aromatic. The higher the amount of naphthene compared to the aromatics indicates the greater conversion of paraffin to naphthene due to the ringing reaction. Based on the reference [17] and the theory of activation energy reduction, as expected, by generating the intermediate naphthenic compound in the dehydrocyclization reaction, the hypothesis of converting paraffin to naphthene is more likely than the direct converting of paraffin to aromatics, and this reaction is done according to the first assumption. And naphthene also becomes aromatic by the reaction of dehydrogenation. Also, by comparing the results of synthetic tests in two different conditions, a decrease in the amount of naphthene and an increase in the number of aromatics in WHSV=1 h^{-1} is observed due to the progression of the naphthene dehydrogenation reaction.

Table 3: Analysis of liquid products in different operating conditions.

T(°C)-P(barg)-H2/Oil-WHSV(hr^{-1})	%mole P	%mole N	%mole A	T(°C)-P(barg)-H2/Oil-WHSV(h^{-1})	%mole P	%mole N	%mole A
Feed	66.24	21.46	11.01				
470-15-6-1	60.67	2.26	36.56	470-10-6-1	58.57	1.7	39.21
480-15-6-1	56.21	1.7	41.53	480-10-6-1	53.76	1.38	44.28
490-15-6-1	50.05	1.27	48.09	490-10-6-1	47.41	1.13	50.85
500-15-6-1	40.89	0.81	57.71	500-10-6-1	38.85	0.88	59.65
470-15-6-2	63.53	2.57	33.33	470-10-6-2	61.99	2.15	35.25
480-15-6-2	60.33	2.09	36.93	480-10-6-2	58.42	1.87	39.03
490-15-6-2	55.78	1.68	41.84	490-10-6-2	53.54	1.61	44.09
500-15-6-2	49.4	1.28	48.57	500-10-6-2	47.01	1.35	50.82
470-15-6-5	66.08	3.56	29.75	470-10-6-5	65.24	3.24	30.83
480-15-6-5	64.33	3.11	31.83	480-10-6-5	63.19	2.98	33.02
490-15-6-5	61.7	2.77	34.71	490-10-6-5	60.22	2.78	36.06
500-15-6-5	57.88	2.42	38.76	500-10-6-5	56.04	2.56	40.33
Synthetic test 470-15-6-1	81.311	10.477	7.397	Synthetic test 470-15-6-5	80.813	14.463	4.228

Table 4 shows the yields of the liquid product process and the outlet flow of hydrogen in different operating conditions. It should be noted that the hydrogen flow at the reactor, entrance is 5.62 g/h.

By examining Table 4, it can be seen that under constant conditions, the rate of yield decreases with increasing temperature, which is due to the effect of cracking the paraffins. As expected, increasing the WHSV parameter or reducing the residence time increases the yield of reformate, as the role of cracking reactions is reduced. An increase in the amount of outlet hydrogen indicates that in this process hydrogen is produced as a byproduct.

Numerical solution of differential equations and modeling results

After presenting the mathematical model and the kinetic model based on their assumptions, it is necessary to use numerical solutions methods of ordinary differential equations to solve it. Therefore, the MATLAB software and the Stiff solution method for ordinary differential equations are used.

In the next step, using the MATLAB optimization tool, the rate constant of each reaction is obtained. The basis of this section is the objective function and in fact the value of the error function. The objective function is defined as $\sum \frac{|y_{model}-y_{exp}|}{y_{exp}}$. Also, the rate constants were extracted from references [5] and [14], and the unit's conversion to the unit in the present model was used as a preliminary guess in optimization. Repeat steps of optimization continue to the extent that the value of the objective function is minimized, and finally, the optimum rate constants are obtained. The rate constant depends on the temperature by the Arrhenius relationship.

$$\mathrm{Lnk} = \mathrm{Lnk}_0 - \frac{\mathrm{E}}{\mathrm{RT}} \quad (3)$$

According to Arrhenius, the rate constant logarithm is linear with 1/T. Therefore, by plotting the diagram of Lnk vs. 1/T in four different temperatures, the kinetic parameters E and Lnk_0 are obtained from the slope of the line and the width from the origin of the graph. The values of these parameters are presented in Table 5.

In reference [14], for each type of reaction, an E value has been reported. In this research, the values of the kinetic parameters are obtained for all the reactions and all the lumps. By comparing the parameter E reported in [14] and its corresponding values in the present model, there is a slight difference between these values.

Table 4: Yields of liquid product and the mass flow rate of the hydrogen output in different operating conditions.

T(°C)-P(barg)-H2/Oil-WHSV(h^{-1})	yield	H_2 (g/h)	T(°C)-P(barg)-H2/Oil-WHSV(h^{-1})	yield	H_2 (g/h)
470-15-6-1	0.914	6.29	470-10-6-1	0.908	6.40
480-15-6-1	0.871	6.30	480-10-6-1	0.869	6.43
490-15-6-1	0.804	6.26	490-10-6-1	0.811	6.42
500-15-6-1	0.701	6.11	500-10-6-1	0.726	6.33
470-15-6-2	0.933	6.24	470-10-6-2	0.926	6.32
480-15-6-2	0.900	6.25	480-10-6-2	0.896	6.35
490-15-6-2	0.849	6.22	490-10-6-2	0.842	6.35
500-15-6-2	0.770	6.13	500-10-6-2	0.781	6.30
470-15-6-5	0.925	6.18	470-10-6-5	0.946	6.23
480-15-6-5	0.934	6.19	480-10-6-5	0.928	6.25
490-15-6-5	0.903	6.18	490-10-6-5	0.899	6.26
500-15-6-5	0.852	6.13	500-10-6-5	0.835	6.23

After examining and precisely in the energy values of the activation, it is concluded that the amounts of this energy for dehydrogenation and dehydrocyclization reactions are lower than other reactions, which also confirms the high rate of these reactions. On the other hand, reactions such as hydrodealkylation and cracking have higher activation energy and hence less rate reaction.

The concentration profile obtained from the kinetic model

After obtaining optimized rate constants, the hydrocarbon concentration profile is obtained under different operating conditions and according to the present model. In this section, the selected hydrocarbon graphs are analyzed at four different temperatures at a pressure 15 bar. In Fig. 2, it can be seen that with increasing temperature, the concentration profile of P_{10} and N_{10} decrease with a more slope and against increase the A_{10} concentration profile with a more slope. This indicates that the rise in temperature leads to the production of more desirable aromatic products, as well as the exacerbation of cracking reactions of paraffins.

It is also seen in Fig. 2 that, with the reduction of the WHSV parameter (increase in reactor length), the amount of aromatic production is increased due to the desirable reactions of dehydrocyclization and dehydrogenation, and the profile has an uptrend. On the other hand, paraffin consumption has increased as a result of cracking reactions, and profiles are on the downside.

In Fig. 3, paraffin P6, which is relatively light paraffin, is associated with increasing concentrations throughout the reactor due to production in heavier paraffins hydrocracking reactions. On the other hand, with increasing temperature, the concentration profile of this hydrocarbon increases with a more slope. However, at 490°C and 500°C, the concentration profile from a cross-sectional dimension reduce the trend. The cause of the descending branch concentration profile of this paraffin at the desired temperature is the consumption in the hydrocracking reaction.

Fig. 4, which is related to light paraffins of 1 to 5 carbon, shows an upward trend in the concentration profiles of these compounds due to the hydrocracking reaction of heavier paraffins and hydrodealkylation reaction. The reported graphs show that the hydrocarbon concentration profile obtained from the model in the given operating conditions has been able to predict the experimental values of the concentration of hydrocarbons in the same conditions.

Fig. 5 shows the magnitude of the difference and error of the concentrations obtained from the model and experimental values. These errors are obtained based on the objective function defined in the optimization phase. Thus, the proposed model, based on the lump hypothesis, can accurately estimate the distribution of products throughout the reactor.

Table 5: Kinetic parameters of the model reactions.

Reactions	E J/mole	k_0 $m^3/kg_{cat}.h$	Reactions	E J/mole	k_0 $m^3/kg_{cat}.h$
$P_{10} \xrightarrow{K1} N_{10} + H_2$	186176	1.52e+12	$N_{10} + H_2 \xrightarrow{K25} P_{10}$	463614	1.83e-34
$P_{10} + H_2 \xrightarrow{K2} P_9 + P_1$	537176	2.58e+36	$N_{10} \xrightarrow{K26} A_{10} + 3H_2$	105222	1.69e+8
$P_{10} + H_2 \xrightarrow{K3} P_8 + P_2$	353403	2.61e+23	$N_9 + H_2 \xrightarrow{K27} P_9$	395879	5.13e-29
$P_{10} + H_2 \xrightarrow{K4} P_7 + P_3$	228053	5.9e+14	$N_9 \xrightarrow{K28} A_9 + 3H_2$	157110	7.30e+11
$P_{10} + H_2 \xrightarrow{K5} P_6 + P_4$	189401	1.16e+12	$N_8 + H_2 \xrightarrow{K29} P_8$	401308	3.30e-29
$P_{10} + H_2 \xrightarrow{K6} 2P_5$	187846	9.99e+11	$N_8 \xrightarrow{K30} A_8 + 3H_2$	61661	1.92e+5
$P_9 \xrightarrow{K7} N_9 + H_2$	229690	1.24e+15	$N_7 + H_2 \xrightarrow{K31} P_7$	140482	1.60e+10
$P_9 + H_2 \xrightarrow{K8} P_8 + P_1$	540019	3.0e+36	$N_7 \xrightarrow{K32} A_7 + 3H_2$	55688	3.16e+4
$P_9 + H_2 \xrightarrow{K9} P_7 + P_2$	331446	1.17e+22	$N_6 + H_2 \xrightarrow{K33} P_6$	385462	4.58e-29
$P_9 + H_2 \xrightarrow{K10} P_6 + P_3$	354476	4.14e+23	$MCP + H_2 \xrightarrow{K34} P_6$	228302	4.36e+15
$P_9 + H_2 \xrightarrow{K11} P_5 + P_4$	259638	8.98e+16	$MCP \xrightarrow{K35} N_6$	229974	5.66e+15
$P_8 \xrightarrow{K12} N_8 + H_2$	275459	1.80e+18	$N_6 \xrightarrow{K36} MCP$	66224	1.04e-5
$P_8 + H_2 \xrightarrow{K13} P_7 + P_1$	462175	7.57e+30	$N_6 \xrightarrow{K37} A_6 + 3H_2$	53373	2.77e+4
$P_8 + H_2 \xrightarrow{K14} P_6 + P_2$	414411	5.53e+27	$A_{10} + 3H_2 \xrightarrow{K38} N_{10}$	114658	1.02e-9
$P_8 + H_2 \xrightarrow{K15} P_5 + P_3$	433675	8.24e+28	$A_{10} + H_2 \xrightarrow{K39} A_9 + P_1$	864548	1.02e-62
$P_8 + H_2 \xrightarrow{K16} 2P_4$	461269	5.32e+30	$A_{10} + H_2 \xrightarrow{K40} A_8 + P_2$	800913	8.52e-59
$P_7 \xrightarrow{K17} N_7 + H_2$	197549	3.60e+12	$A_{10} + H_2 \xrightarrow{K41} A_7 + P_3$	1148953	2.99e-83
$P_7 + H_2 \xrightarrow{K18} P_6 + P_1$	251399	7.93e+15	$A_9 + 3H_2 \xrightarrow{K42} N_9$	154624	9.77e-13
$P_7 + H_2 \xrightarrow{K19} P_5 + P_2$	772570	4.05e+51	$A_9 + H_2 \xrightarrow{K43} A_8 + P_1$	234529	5.50e-19
$P_7 + H_2 \xrightarrow{K20} P_4 + P_3$	429485	2.36e+28	$A_9 + H_2 \xrightarrow{K44} A_7 + P_2$	296169	2.09-23
$P_6 \xrightarrow{K21} N_6 + H_2$	147191	7.99e+8	$A_8 + 3H_2 \xrightarrow{K45} N_8$	136624	3.04e-11
$P_6 + H_2 \xrightarrow{K22} P_5 + P_1$	210086	1.15e+13	$A_8 + H_2 \xrightarrow{K46} A_7 + P_1$	262315	4.13e-21
$P_6 + H_2 \xrightarrow{K23} P_4 + P_2$	325909	7.12e+20	$A_7 + 3H_2 \xrightarrow{K47} N_7$	132949	4.84e-11
$P_6 + H_2 \xrightarrow{K24} 2P_3$	370015	7.44e+23	$A_6 + 3H_2 \xrightarrow{K48} N_6$	109296	2.11e-9

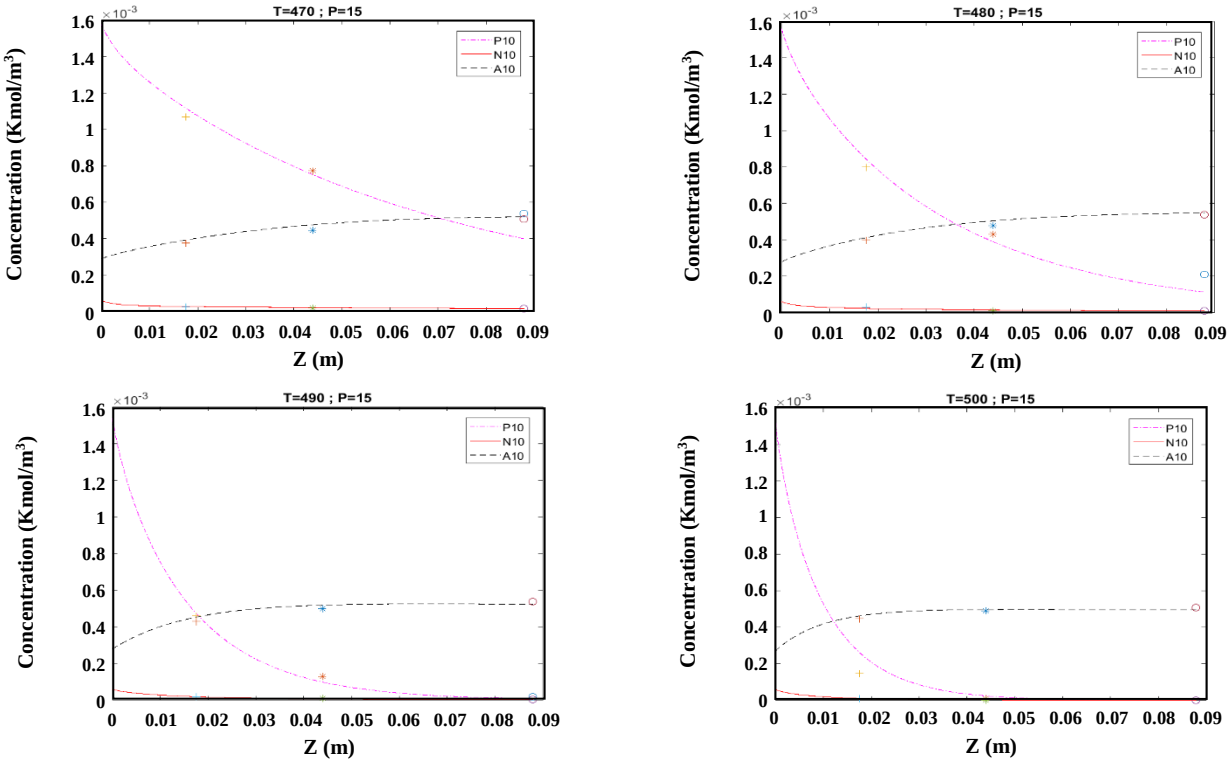

*Fig. 2: Hydrocarbon C_{10} concentration profiles and comparison with experimental values (○ in WHSV=1 h^{-1}, * in WHSV=2 h^{-1}, + in WHSV=5 h^{-1}); Pressure in 15 barg; Temperature in a)470°C, b)480°C, c)490°C, d)500°C.*

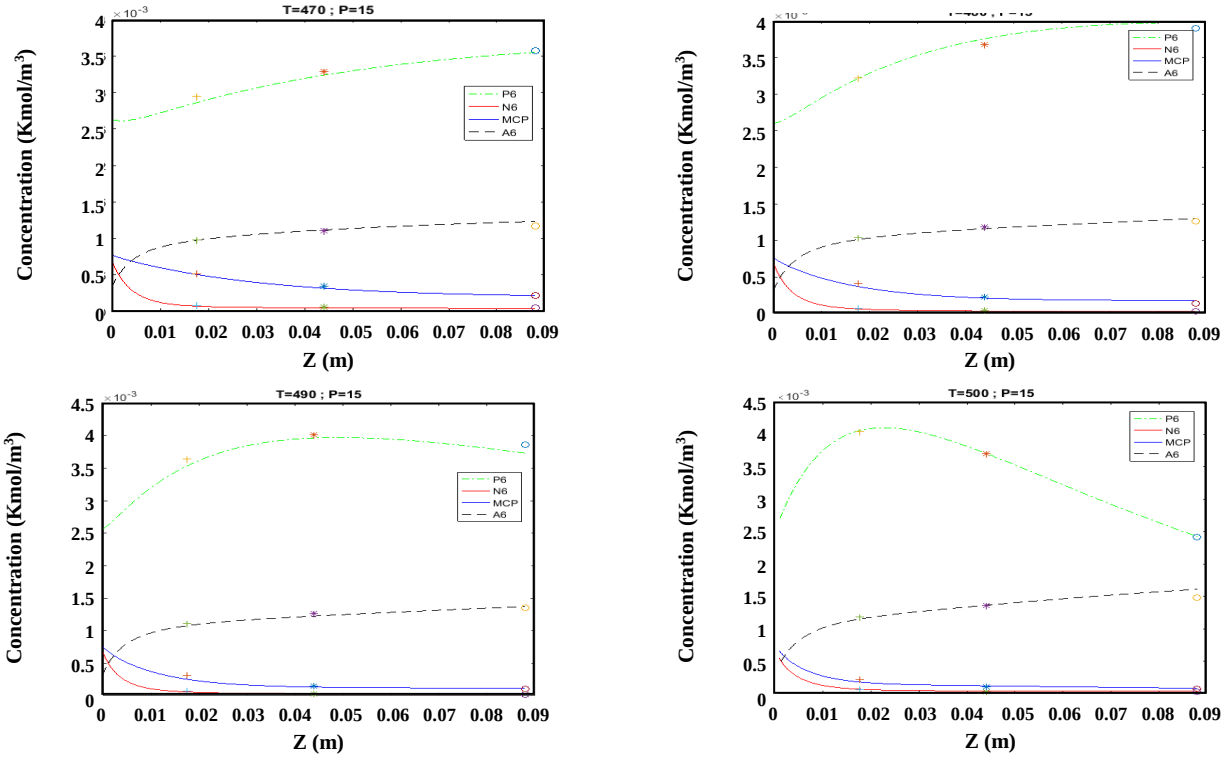

*Fig. 3: Hydrocarbon C_6 concentration profiles and comparison with experimental values (○ in WHSV=1 h^{-1}, * in WHSV=2 h^{-1}, + in WHSV=5 h^{-1}); Pressure in 15 barg; Temperature in a)470°C, b)480°C, c)490°C, d)500°C.*

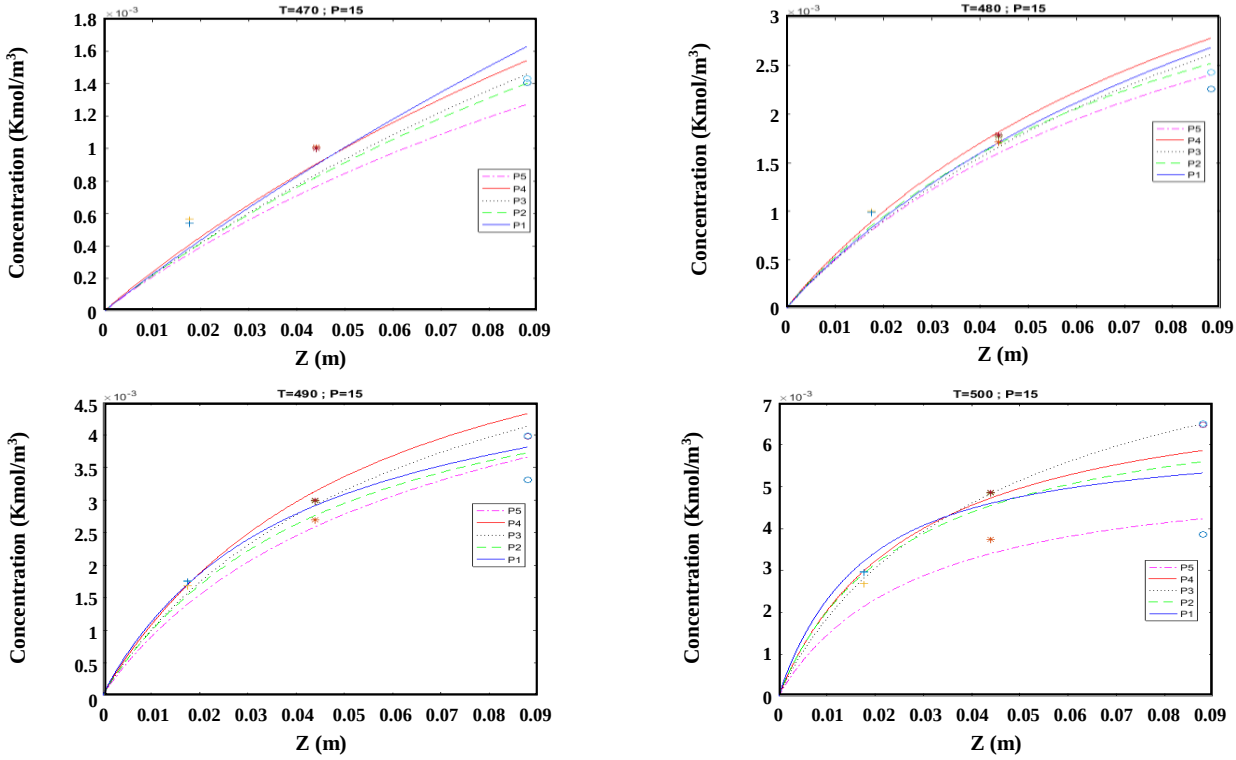

*Fig. 4: Hydrocarbon C_1-C_5 concentration profiles and comparison with experimental values (○ in WHSV=1 hr^{-1}, * in WHSV=2 hr^{-1}, + in WHSV=5 hr^{-1}); Pressure in 15 barg; Temperature in a)470°C, b)480°C, c)490°C, d)500°C.*

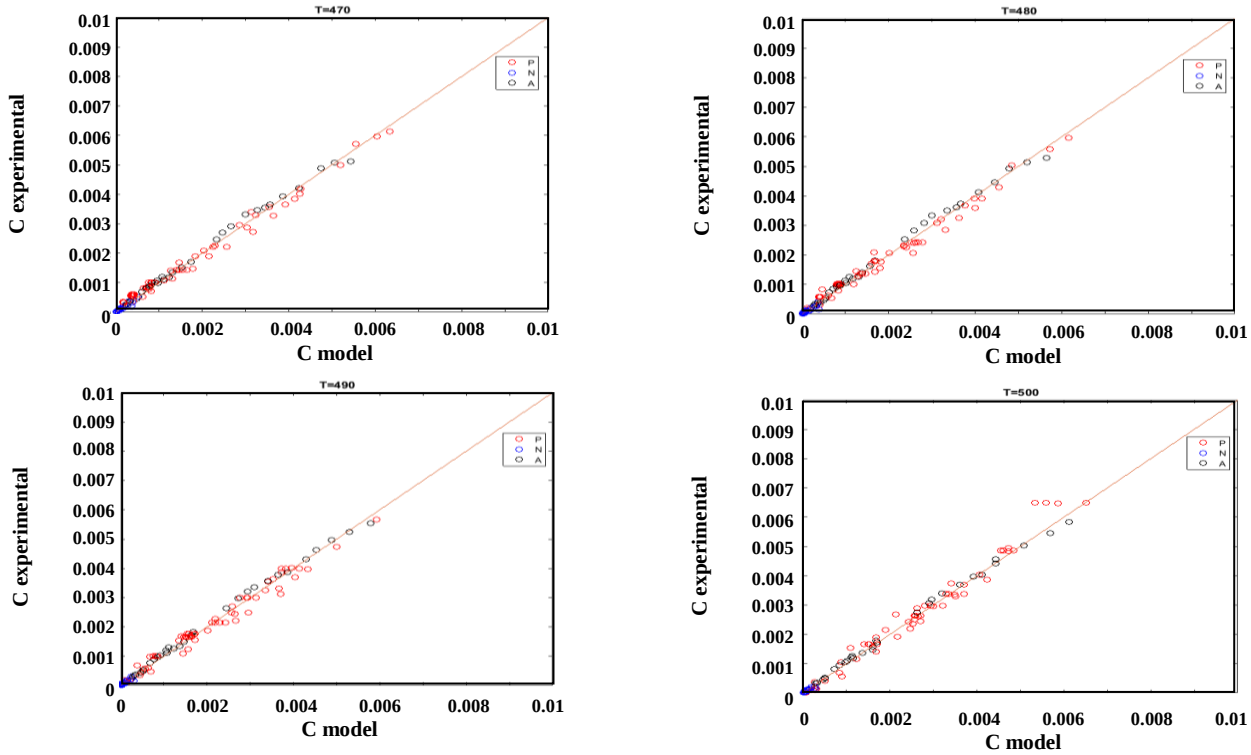

Fig. 5: Difference of concentration values obtained from the model with experimental values; Pressure in 15 barg; The temperature in a)470°C, b)480°C, c)490°C, d)500°C.

Table 6: Predicted superficial velocity of output fluid from reactor in different operating conditions.

T(°C)-P(barg)-H2/Oil-WHSV(hr^{-1})	U_0(m/hr)	U_e(m/hr)	T(°C)-P(barg)-H2/Oil-WHSV(hr^{-1})	U_0(m/hr)	U_e(m/hr)
470-15-6-1	16.035	18.242	490-15-6-1	16.467	19.161
470-15-6-2	16.035	17.837	490-15-6-2	16.467	18.793
470-15-6-5	16.035	17.487	490-15-6-5	16.467	18.319
470-10-6-1	24.05	26.974	490-10-6-1	24.70	28.422
470-10-6-2	24.05	26.488	490-10-6-2	24.70	27.864
470-10-6-5	24.05	26.014	490-10-6-5	24.70	27.179
480-15-6-1	16.251	18.739	500-15-6-1	16.683	19.685
480-15-6-2	16.251	18.302	500-15-6-2	16.683	19.403
480-15-6-5	16.251	17.870	500-15-6-5	16.683	18.895
480-10-6-1	24.377	27.710	500-10-6-1	25.024	29.301
480-10-6-2	24.377	27.142	500-10-6-2	25.024	28.789
480-10-6-5	24.377	26.548	500-10-6-5	25.024	27.963

The variable superficial velocity of the fluid

One of the important assumptions of the model is the variable velocity of fluid flow inside the reactor. Following the implementation of the model, the results of the superficial velocity of the fluid in the reactor, in various operating conditions, are given in Table 6.

According to Table 6, the output velocity is 11-17% more than the input velocity, which reduces the actual residence time of the reactor relative to its superficial residence time. According to the residence time relation $\tau = V / U.A_z$, with increasing the velocity, the residence time decreases, and in the constant volume of the reactor, the conversion rate decreases. Therefore, in order to achieve a certain degree of conversion, a larger volume of the reactor is needed. If the variable velocity hypothesis is not considered in the modeling, then it is not possible to correctly design the reactor size and the amount of catalyst. In this case, the importance of the hypothesis of the variable velocity of the fluid, especially in reactor modeling, is determined.

CONCLUSIONS

In this research, a kinetic model based on the lump hypothesis has been developed for the chemical reactions of the naphtha catalytic reforming process. This model is presented in the form of 22 lumps and 48 reactions. After the numerical solution of the differential equations of the model using the results of the product analysis and optimization of the rate constant with the software of MATLAB, the kinetic parameters E and k_0 were obtained. Finally, the concentration profiles obtained from the model for hydrocarbons throughout the reactor were compared and verified with their corresponding experimental values in different operating conditions. After examining these diagrams, it can be concluded that this model has been able to accurately predict the distribution of products throughout the reactor. Considering the variable fluid velocity in the reactor, 11-17% rise in output velocity is emerged. This issue is impressive for obtaining actual residence time and reactor design size.

Nomenclature

A_z	Cross-section area of reactor in radial direction, m^2
a_s	Surface area of catalyst, m^2/g
C_j	Concentration of *j*th component, $kmol/m^3$
d_p	Particle diameter, m
E	Activation energy, J/kmol
i	Numerator for reaction
j	Numerator for component
k	Reaction rate constant for reaction, $m^3/kg_{cat}/h$
k_0	Frequency factor, $m^3 / kg_{cat}.h$
m	Number of reactions
n	Number of components
P	Total pressure, kPa
r	Radius, m
r_i	Rate of *i*th reaction, $kmol/kg_{cat}.h$

R	Gas constant, J/mol.K
T	Temperature, K
U	Fluid velocity in reactor, m/h
U_0	Superficial velocity of fluid in entrance of reactor, m/h
Ue	Superficial velocity of fluid in exit of reactor, m/h
U_z	Superficial velocity of fluid in reactor in axial direction, m/h
V	Volume of reactor, m^3
v_p	Total pore volume, cm^3/g
WHSV	Weight hourly space velocity, h^{-1}
z	Length of reactor, m
v_{ij}	Stoichiometric coefficient of component *j* in reaction *i*
ρ_B	Reactor bed density, kg/m^3
τ	Residence time, h

Received : Aug. 1, 2019 ; Accepted :Oct. 21, 2019

REFERENCES

[1] Rahimpour M.R., Jafari M., Iranshahi D., Progress in Catalytic Naphtha Reforming Process: A Review, *Appl. Energy*, **109**: 79–93 (2013).

[2] Leprince P., Martino G., "Petroleum Refining, Conversion Processes", 3rd ed., Technip (2001).

[3] Antons G.J., Aitani A., "Catalytic Naphtha Reforming". Marcel Dekker, New York, (1981).

[4] Nabgan W., Rashidzadeh M., Nabgan B., The Catalytic Naphtha Reforming Process: Hydrodesulfurization, Catalysts and Zeoforming, *Environ. Chem. Lett*., 1–16 (2018).

[5] Rodríguez M.A., Ancheyta J., Detailed Description of Kinetic and Reactor Modeling for Naphtha Catalytic Reforming, *Fuel*, **90**: 3492–3508 (2011).

[6] Dachos N., Kelly A., Felch D., Reis E., UOP Platforming Process. In Handbook of Petroleum Refining Processes, 2nd ed. McGraw-Hill, New York (1997).

[7] Iranshahi D., Hamedi N., Nategh M., Saeedi R., Saeidi S., Thermal Integration of Sulfuric Acid and Continuous Catalyst Regeneration of Naphtha Reforming Plants, *Chem. Eng. Technol*., 1–36 (2017).

[8] Taskar U., "Modeling and Optimization of a Catalytic Naphtha Reformer", Texas Tech University (1996).

[9] Sa'idi M., Mostoufi N., Sotudeh-Gharebagh R., Modelling and Optimisation of Continuous Catalytic Regeneration Process Using Bee Colony Algorithm, *Can. J. Chem. Eng*., **91**: 1256–1269 (2013).

[10] Babaqi B.S., Takriff M.S., Kamarudin S.K., Othman N.T.A., Mathematical Modeling, Simulation, and Analysis for Predicting Improvement Opportunities in the Continuous Catalytic Regeneration Reforming Process, *Chem. Eng. Res. Des*., **132**: 235–251 (2018).

[11] Turaga U.T., Ramanathan R., Catalytic naphtha Reforming: Revisiting its Importance in the Modern Refinery, *J. Sci. Ind. Res.* (India), **62**: 963–978 (2003).

[12] Iranshahi D., Karimi M., Amiri S., Jafari M., Rafiei R., Rahimpour M.R., Modeling of Naphtha Reforming Unit Applying Detailed Description of Kinetic in Continuous Catalytic Regeneration Process, *Chem. Eng. Res. Des*., **92**: 1704–1727 (2014).

[13] Smith R., Kinetic Analysis of Naphtha Reforming with Platinum Catalyst, *Chem Eng Prog*., **55**: 76–80 (1959).

[14] Krane H.G., Groh A.B., Schuhnan B.L., Sinfeh J.H., "Reactions in Catalytic Reforming of Naphthas", in: *5th WorldPetroleum Congress*,. New York (1959).

[15] Padmavathi G., Chaudhuri K.K., Modeling and Simulation of Commercial Catalytic Naphtha Reformers, *Can. J. Chem. Eng.*, **75**: 930–937 (1997).

[16] Zagoruiko A.N., Belyi A.S., Smolikov M.D., Noskov A.S., Unsteady-State Kinetic Simulation of Naphtha Reforming and Coke Combustion Processes in the Fixed and Moving Catalyst Beds, *Catal. Today*, **220–222**: 168–177 (2014).

[17] Mcmurry J., "Organic Chemistry", 9th ed. Cengage Learning, Boston,USA (2016).